Monitoring of "Urban Villages" in Shenzhen, China from High-Resolution GF-1 and TerraSAR-X data

Chunzhu Wei*[a], Thomas Blaschke[a], Hannes Taubenböck[b]

[a]Department of Geoinformatics - Z_GIS, University of Salzburg, Schillerstrasse 30, 5020 Salzburg, Austria; [b]German Aerospace Center (DLR), German Remote Sensing Data Center, Oberpfaffenhofen, 82234 Weßling, Germany

ABSTRACT

Urban villages comprise mainly low-rise and congested, often informal settlements surrounded by new constructions and high-rise buildings whereby structures can be very different between neighboring areas. Monitoring urban villages and analyzing their characteristics are crucial for urban development and sustainability research. In this study, we carried out a combined analysis of multispectral GaoFen-1 (GF-1) and high resolution TerraSAR-X radar (TSX) imagery to extract the urban village information. GF-1 and TSX data are combined with the Gramshmidt spectral sharpening method so as to provide new input data for urban village classification. The Grey-Level Co-occurrence Matrix (GLCM) approach was also applied to four directions to provide another four types (all, 0°, 90°, 45° directions) of TSX-based inputs for urban village detection. We analyzed the urban village mapping performance using the Random Forest approach. The results demonstrate that the best overall accuracy and the best producer accuracy of urban villages reached with the GLCM 90° dataset (82.33%, 68.54% respectively). Adding single polarization TSX data as input information to the optical image GF-1 provided an average product accuracy improvement of around 7% in formal built-up area classification. The SAR and optical fusion imagery also provided an effective means to eliminate some layover, shadow effects, and dominant scattering at building locations and green spaces, improving the producer accuracy by 7% in urban area classification. To sum up, the added value of SAR information is demonstrated by the enhanced results achievable over built-up areas, including formal and informal settlements.

Keywords: Urban villages, GF-1, TerraSAR-X, Image fusion, Random Forest

1. INTRODUCTION

Informal settlements are a world-wide phenomenon, and the monitoring and modeling of informal settlements is crucial for the understanding of slum genesis and development in general. Many previous studies that applied the VHR optical data have been conducted to detect and analyze informal settlements, (e.g.Graesser et al. 2012; Esch et al. 2012; Netzband and Rahman 2009; Hofmann et al. 2008), but not many have used SAR data to discuss the urban environment issue when compared with the optical data (Gamba, Aldrighi, and Stasolla 2010; Stasolla and Gamba 2008). For the Chinese version of the informal settlement phenomenon of urban villages, there is still no definitive spatial description or a general systematical definition on such locations based on optical and SAR data.

SAR systems are highly attractive due to their independence of daytime and weather. Radar data has undoubtedly led to a new era for acquiring geographical coverage information (Brunner, Lemoine, and Bruzzone 2010; Soergel et al. 2006). Especially since the launch of TerraSAR-X, the new satellite configuration of TerraSAR-X and TanDEM-X provide single-pass 3D mapping of the earth with unprecedented geometric resolution, allowing for improved detection and extraction of building positions and shapes (Gernhardt et al. 2010, Baghdadi et al., 2009; Breidenbach et al.,2010; Burini et al., 2008; Mro′ z and Mleczko, 2008). Nevertheless, high resolution TerraSAR-X imagery has thus far barely been employed for dense informal settlements areas, such as urban village analysis (Taubenböck and Kraff 2013, Reigber et al. 2007). An improvement of classification accuracy has been achieved for both multispectral optical data and radar imagery (Mahmoud et al. 2011). The integration of SAR images with optical imageries has improved the classification of build-up areas by enhancing certain features, improving geometric correction, and so on (Amarsaikhan et al. 2007; Blaes, Vanhalle, and Defourny 2005). Many previous studies indicated that the fusion of SAR and optical imagery can effectively take into consideration the impact of the phenomena layover, shadow, and dominant scattering at building location (Blaes, Vanhalle, and Defourny 2005; Stilla, Soergel, and Thoennessen 2003). Especially when the SAR

SAR Image Analysis, Modeling, and Techniques XV, edited by Claudia Notarnicola, Simonetta Paloscia, Nazzareno Pierdicca, Proc. of SPIE Vol. 9642, 964210
 · doi: 10.1117/12.2194877

images are corrupted by speckle, noise effect, and the lack of bands, combining optical imageries with SAR data may be efficiently used for an improved building structure information extraction.

The overall objective of this research is to develop an innovative framework for combined analysis of multi-spectral image GaoFen-1(GF) and single-polarization TSX imagery in urban village monitoring. We want to test and compare the performance of different inputs (including optical image GF-1, the fusion images of GF-1 and TSX, and texture features of TSX) in classifying urban villages, in order to maximize the classification accuracy from the integration of GF-1 and SAR images.

2. STUDY AREA AND DATA COLLECTION

Shenzhen is one of the most densely populated, most populous, rapidly commercialized and urbanized economic regions in China, with a population of 12 to 15 million people. There is a unique urban growth phenomenon called 'urban village' that has appeared in this area. Urban villages are the by-products of the rapid urbanization in Shenzhen, where the city develops around what once were isolated farming and fishing villages. They are surrounded by skyscrapers, transportation infrastructures, and other modern urban constructions, and there are around 6 million residents living in such informal settlements. The test area in this study mainly covers the Baoan district, over a subset area of nearly 480 km^2, in the South-West of the city of Shenzhen.

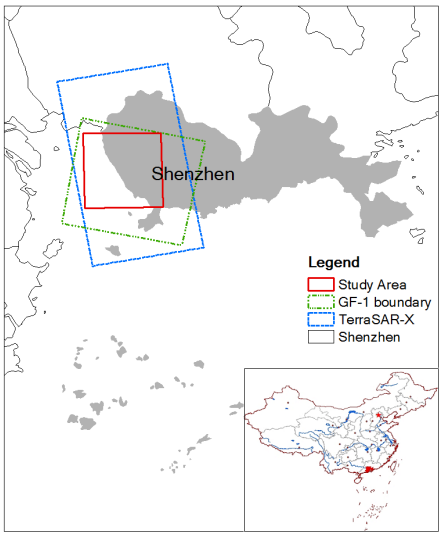

Figure 1. Study area and dataset cover area overview

Gaofen-1 (Gao Fen = high resolution) is the first of a series of high-resolution optical Earth observation satellites of the CNSA (China National Space Administration), Beijing, China. This satellite aims to provide Near-Real-Time (NRT) observations for geographical mapping of the environment. In our study, one GF-1 PMS image (8×8 meter resolution), which was acquired on the 25th of December 2013, was chosen as the optical image to do the urban village classification. The four CCD reflective bands of GF-1 range from 0.45 μm to 0.89 μm. For SAR data, one TSX map (SM mode, HH polarization, orbit cycle 189, and 3×3 meter spatial resolution) was acquired on the 24th of February 2013.

3. METHODOLOGY

3. 1 Work flow and Preprocessing

Due to the speckle noise effect and the lack of full bands information, the interpretation of single-polarization SAR images with optical images is still an interesting but difficult topic. We thus proposed a hybrid multi-process GF-1&TSX cooperation model to integrate high resolution optical images and single-polarization SAR information. Figure 2 summarizes the overall analysis procedure, which was a progressive process comprised of four main stages. Initially, all the pre-processed steps were needed for optical data and TSX data. Then, in order to ascertain whether the TSX information is important to improving the analysis, the optical and SAR image fusion analysis, and TSX-based texture features analysis were implemented separately for further classification. Last but not least, the Random Forest approach

was adopted to carry out the urban village classification, compare its accuracy, and assess the potential benefits and tradeoffs.

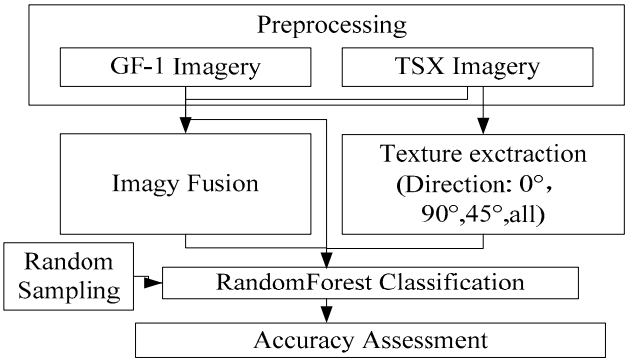

Figure 2. Flowchart of urban village classification

Pre-processed of TSX was carried out using ESA-NEST software. The TSX image was firstly geocoded to WGS84-UTM 49N. The image was subsequently radiometric calibrated to Sigma Nought (σ°), which represents the radar reflectivity per unit area in the ground range by using elevation data from a SRTM DEM. The speckle filtering approach Lee was used to reduce the speckle noise in the original SAR image. Finally, the intensity band was translated to the visual band to conduct the further analysis. For the pre-processing of GF-1, all the bands required radiometric calibration, whereby the original digital numbers (DN) of the images were converted to exo-atmospheric reflectance. Radiometric calibration and atmospheric correction of GF-1 image were carried out based on the HJ-1A/1B tools V3.0 and FLAASH Atmospheric Correction Model in ENVI.

3.2 Image fusion

The characteristics of data acquired by optical and synthetic aperture radar (SAR) sensors greatly differ. Multispectral satellites provide information from the visible to the thermal infrared. SAR sensors provide measurements in amplitude and phase related to the interaction of the Earth's surface with microwaves. SAR sensors thus provide information that may not be obtained from optical sensors (Kim et al. 2011). In order to improve results in the classification process compared to the conventional multi-spectral image, we used image fusion to generate a new image by integrating different spatial and spectral characteristics of the images. Image fusion is wildly used to provide detailed input to the image classification. In many prior studies, the Gramshmidt spectral sharpening method performed better than other methods, such as the Principle Component Spectral Sharpening (GF), the Least Square Fusion, and so on (Ozdarici Ok and Akyurek 2012; Pohl and Genderen 1998). In this study, the performance of GS was presented based on the multispectral GF-1 image and the TSX HH band image. Two source images were georeferenced to a standard map projection. We used ENVI to performan GS by simulating the GF-1 multi-spectral band from the lower spatial spectral bands, and swapping the high spatial resolution band with the first GS band.

3.3 Textural analysis

More recently, texture measures such as the co-occurrence measures according to Haralick (1973) have already shown their potential for extracting information on urban environments and enhancing classification performance using SAR data (Espinoza Molina, Gleich, and Datcu 2012; Mather and Tso 2009; Haralick, Shanmugam, and Dinstein 1973). In our study, one of the most prevalent techniques, the Grey-Level Co-occurrence Matrix (GLCM), was used to derive textural characteristics. These features were imported as new layers and implemented as new data for the Random Forest prior classifier training. The texture features that we computed are: GLCM mean, GLCM standard deviation, GLCM homogeneity, GLCM correlation, GLCM contrast, GLCM ang. 2nd moment, GLCM dissimilarity, GLCM entropy.

3.3 Classification

The popular supervised classification algorithm 'Random Forest' was applied to the different groups of multi-source and multi-spectral satellite datasets mentioned above in order to produce an urban village map. Random Forest (RF) is a ensemble learning classifier that consists of a number of trees to produce a classification output on the basis of the majority voting principle (Sonobe et al. 2014). In this study, the imageRF tool in the EnMAP-Box software was used to implement the Random Forest classification (Waske et al. 2012). Four types of land use and land cover information were

taken into consideration: urban areas, urban villages, vegetation, and water. We estimated categorical or continuous variables for different groups of images by setting up 500 self-learning decision tress to parameterize the model (Ma et al. 2012). In order to ensure the reliability of the results, we divided our data into a training and a validation data set. Around 3000 Training samples and 3000 validation samples for each land use type were extracted using stratified equalized random sampling.

4. RESULTS AND DISCUSSION

Urban village extraction maps based on multi-resource data are listed in Figure 2. As Table 1 shows, RF performed best in the GLCM 90° dataset, with an overall accuracy of 82.33%, and a Kappa accuracy of 0.76. The performance of the textural feature groups GLCM all, 0, 45 were quite similar, with their overall accuracies ranging from 80.87-80.86%, followed by the GF-1+TSX image fusion dataset, with an overall accuracy of 79.98%. The GF-1 image performed worst in urban village classification with an overall accuracy of 79.1% and a Kappa of 0.72.

Table 2 demonstrates the producer accuracies of the four classes. The analysis of results achieved by TSX texture features showed that urban village maps produced through GLCM 90° granted an accuracy increment of 5.8% in producer accuracy with the Radom Forest algorithm (Figure 2d) compared with the base image scenario using only GF-1 as input. An average increase of 5% in producer accuracy was observed in all types of GLCM datasets. The same occurred in the classification of urban areas mainly comprising the formal settlement areas. Compared with the urban village map produced by using only GF-1, adding the TSX information granted an absolute accuracy increment of 7% (GF-1+TSX) to 15% (GLCM) in producer accuracy. Looking at the class error highlighted in the graphs of Figure 2, we observed that in the northwestern part of Shenzhen, GF-1 data and the image fusion data show an obvious overestimation in urban village classification. These areas are the newly developing areas under urban expansion. Most of them are industrial buildings with a homogeneous distribution and low height. Therefore, it is not easy to distinguish the urban villages and the industrial zones based on spectral bands information. By contrast, in the southeastern part of Shenzhen, the dataset of all GLCM features (Figure e to Figure f) show an overestimation in the urban village classification based on TSX data. These areas are the city center of Shenzhen, where most of the skyscrapers are located. Even if some urban villages still exist in the city center, the textural features of the TSX cannot distinguish the urban villages and other types of informal settlement areas that are unregularly distributed and dispersed due to the influence of the continuous alteration of layover and the shadow areas coming from tall building. In general, the TSX textural features group GLCM 90° , GLCM 0° ,GLCM 45° ,GLCM all performed better than GF-1 and GF-1+TSX groups in classifying the large areas of informal settlements. Their classification results are more clustered and the results derived from the GF-1 image (Figure 2a) and GF+TSX image (Figure 2b) correspond well with the spatial distribution of urban villages. Both the TSX texture information and the GF-1+TSX fusion image obviously enhance the producer accuracy of formal settlements compared with GF-1 data.

The optical image and TSX image both have advantages and disadvantages in classifying other variety classes. In terms of vegetation classification, because of the noise influence in the TSX data, adding textural features to the classification input strongly diminished the classification error for trees and grass classification, as can be seen in the northwestern parts of Figure 2c to Figure 2f. These types of vegetation areas are mainly located in the streets or other densely built-up areas. Their classifications are easily influenced by the shadow of tall buildings or the mixed-pixel problem. Nevertheless, the classification results from the GLCM dataset also show more noise points or errors in the vegetation areas when compared with the GF-1 image and the GF+TSX image, causing a slight decrement (around 1% to 3%) of producer accuracy in vegetation class classification compared with optical image and GF+TSX image. In terms of water classification, compared with the image fusion group, some uncompleted classification also occurs in the GF-1 images (Figure 2a), as well as errors in the GLCM feature groups (Figure 2c-Figure 2f), which indicates that the combination of the optical image and SAR data can deal with the mixed-pixel problems that exist in the optical image to some extent. We can thus come to the conclusion that the classes which showed sensible discrimination issues using only optical features belong to the vegetation class and water class, especially when using only the optical image as input. The image classification from the image fusion dataset input contributed to decreasing the errors for the build-up class and vegetation class compared with the optical image. The noise problem in TSX data also needs to be considered in the vegetation classification.

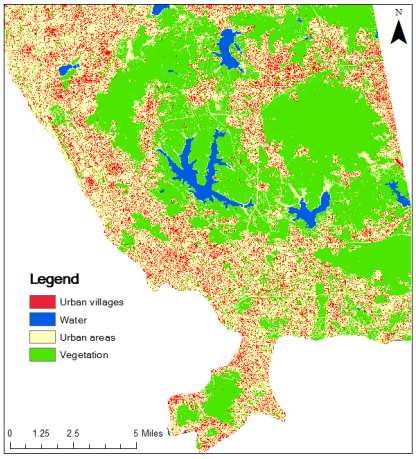

Figure a. GF-1

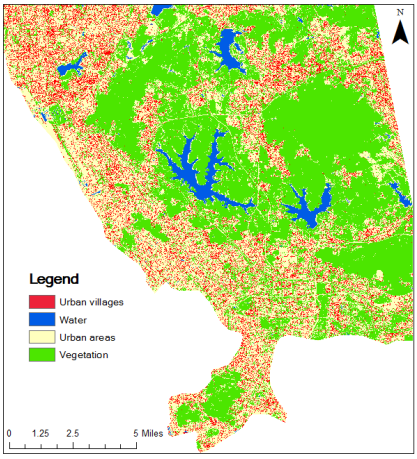

Figure b. GF+TSX image

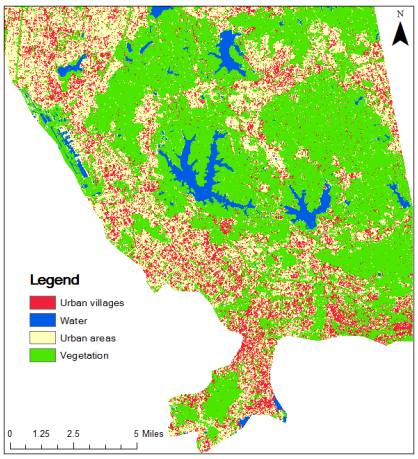

Figure c. GLCM 0°

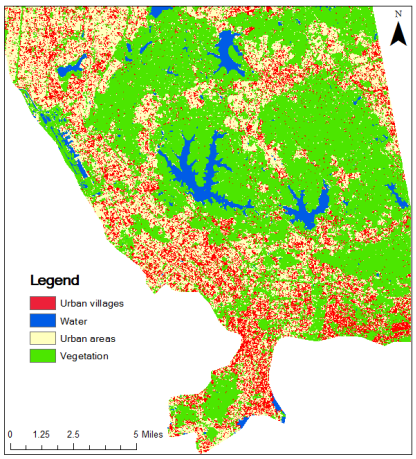

Figure d. GLCM 90°

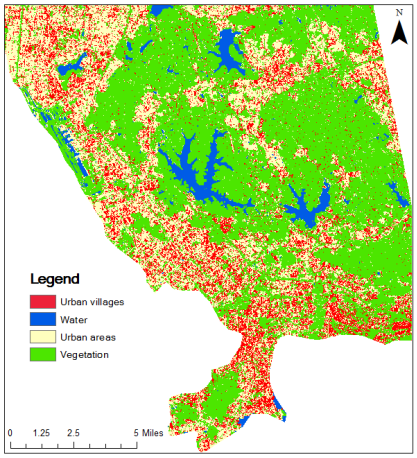

Figure e. GLCM 45°

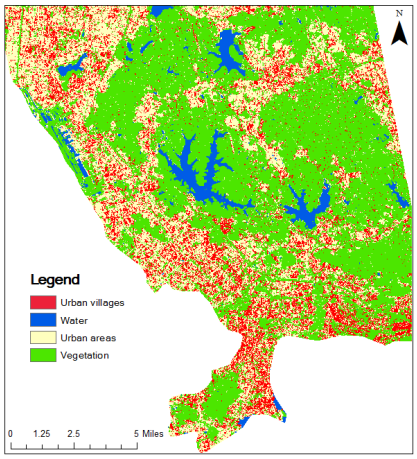

Figure f. GLCM all

Figure. 2. Urban villages extraction map derived through Random Forest algorithm using different input features: (a) GF-1 image, (b) GF+TSX, (c) GLCM 0°, (d) GLCM 90°,(d) GLCM 45°,(d) GLCM all

Table 1. Overall accuracy of urban village maps

	GF-1 (%)	GF-1+TSX (%)	GLCM All (%)	GLCM 90° (%)	GLCM 45° (%)	GLCM 0° (%)
Overall accuracy	79.10	79.98	80.96	82.33	80.87	80.97
Kappa	0.72	0.73	0.75	0.76	0.74	0.75

Table 2. Producer accuracy of urban village maps

	GF-1 (%)	GF-1+TSX (%)	GLCM All (%)	GLCM 90° (%)	GLCM 45° (%)	GLCM 0° (%)
Urban villages	62.74	61.46	67.96	68.54	67.74	68.18
Urban areas	70.98	77.50	85.10	85.21	85.17	85.10
Vegetation	99.52	99.65	96.96	98.62	96.85	96.82
Water	82.02	80.15	72.52	75.71	72.40	72.48

5. CONCLUSION

This paper has presented a framework for urban village extraction through the integration of high resolution optical image GF-1 data and TSX data. The Random Forest algorithm was applied to three types of multi-resource datasets: GF-1 optical image, GF-1+TSX image, and GLCM data from TSX. The comparison of multi-resource urban village mapping was carried out with the spectral information and textural features. The results demonstrated that the best overall accuracy was reached with the GLCM texture features using Random Forest. Adding TSX texture features as input information led to a 2% absolute increment in overall accuracy. The GLCM texture information from the TSX image performed well in informal settlement mapping, even if some of the informal settlements do not belong to the urban villages. In addition, TSX data was shown to be advantageous in mapping formal settlement areas and small-scale vegetation corridors compared with optical images. However, the noise problem in TSX also influences its application in classifying small-scale built-up areas. The GF-1+TSX image also performed better than the optical image in urban areas and vegetation areas classification while the classification accuracies of urban village were similar. Overall, adding the TSX data was significant importance since the texture feature input or fusion image input all enhance the overall accuracy of urban villages mapping in the city of Shenzhen, China. The informal settlements, most of which represent urban villages, still exist in many areas of Shenzhen, and hinder the sustainable development of urbanization. The classification results in our study not only provide new insights for analyzing the heterogeneity of the spatial characteristic of urban villages, but also validate the advanced capabilities of high resolution GF-1 data and TSX data in informal settlement mapping.

ACKNOWLEDGEMENTS

The TerraSAR-X data used for the analysis were provided by German Aerospace Center-DLR in the framework of the scientific proposal LAN2927. The GF-1 data used for the analysis was provided by the Institute of Remote Sensing Application Chinese Academy of Science.

REFERENCES

[1] Amarsaikhan, D., M. Ganzorig, P. Ache, and H. Blotevogel. "The Integrated Use of Optical and InSAR Data for Urban Land‐cover Mapping," International Journal of Remote Sensing 28 (6), 1161‐71 (2007).

[2] Blaes, Xavier, Laurent Vanhalle, and Pierre Defourny. "Efficiency of Crop Identification Based on Optical and SAR Image Time Series," Remote Sensing of Environment 96 (3–4), 352–65 (2005).

[3] Brunner, D., G. Lemoine, and L. Bruzzone. "Earthquake Damage Assessment of Buildings Using VHR Optical and SAR Imagery," IEEE Transactions on Geoscience and Remote Sensing 48 (5), 2403–20 (2010).
[4] Esch, Thomas, Hannes Taubenböck, Achim Roth, Wieke Heldens, Andreas Felbier, Michael Thiel, Martin Schmidt, Andreas Müller, and Stefan Dech. "TanDEM-X Mission—new Perspectives for the Inventory and Monitoring of Global Settlement Patterns," Journal of Applied Remote Sensing 6 (1), 061702–1 (2012).
[5] Espinoza Molina, D., D. Gleich, and M. Datcu. "Evaluation of Bayesian Despeckling and Texture Extraction Methods Based on Gauss,Markov and Auto-Binomial Gibbs Random Fields: Application to TerraSAR-X Data." IEEE Transactions on Geoscience and Remote Sensing 50 (5), 2001–25 (2012).
[6] Gamba, P., M. Aldrighi, and M. Stasolla. "Robust Extraction of Urban Area Extents in HR and VHR SAR Images," IEEE Journal of Selected Topics in Applied Earth Observations and Remote Sensing 4 (1), 27–34 (2011).
[7] Gernhardt, S., N. Adam, M. Eineder, and R. Bamler. "Potential of Very High Resolution SAR for Persistent Scatterer Interferometry in Urban Areas," Annals of GIS 16 (2), 103–11 (2010).
[8] Graesser, J., A. Cheriyadat, R.R. Vatsavai, V. Chandola, J. Long, and E. Bright. "Image Based Characterization of Formal and Informal Neighborhoods in an Urban Landscape," IEEE Journal of Selected Topics in Applied Earth Observations and Remote Sensing 5 (4), 1164–76 (2012).
[9] Amarsaikhan, D., M. Ganzorig, P. Ache, and H. Blotevogel. "The Integrated Use of Optical and InSAR Data for Urban Land‐cover Mapping," International Journal of Remote Sensing 28 (6), 1161‐1171 (2007).
[10] Hofmann, P., J. Strobl, T. Blaschke, and H. Kux. "Detecting Informal Settlements from QuickBird Data in Rio de Janeiro Using an Object Based Approach." Object-Based Image Analysis, Springer Berlin Heidelberg, 531–538 (2008).
[11] Kim, Yonghyun, Changno Lee, Dongyeob Han, Yongil Kim, and Younsoo Kim. "Improved Additive-Wavelet Image Fusion," IEEE Geoscience and Remote Sensing Letters 8 (2),263–67 (2011).
[12] Ma, Le, Hong-Liang Dou, Yi-Qun Wu, Yang-Mu Huang, Yu-Bei Huang, Xian-Rong Xu, Zhi-Yong Zou, and Xiao-Ming Lin. "Lutein and Zeaxanthin Intake and the Risk of Age-Related Macular Degeneration: A Systematic Review and Meta-Analysis," British Journal of Nutrition 107 (03), 350–59 (2012).
[13] Mahmoud, Ali, Samy Elbialy, Biswajeet Pradhan, and Manfred Buchroithner. "Field-Based Landcover Classification Using TerraSAR-X Texture Analysis," Advances in Space Research 48 (5), 799–805 (2011).
[14] Mather, Paul, and Brandt Tso. Classification Methods for Remotely Sensed Data, Second Edition. CRC Press, 221-252 (2009).
[15] Netzband, M., and A. Rahman. "Physical Characterisation of Deprivation in Cities: How Can Remote Sensing Help to Profile Poverty (slum Dwellers) in the Megacity of Delhi/India," In Urban Remote Sensing Event, 2009, 1–5 (2009)
[16] Ozdarici Ok, A., and Z. Akyurek. "Automatic Training Site Selection for Agricultural Crop Classification: a Case Study on Karacabey Plain," ISPRS - International Archives of the Photogrammetry, Remote Sensing and Spatial Information Sciences 19(4), 221–25 (2012).
[17] Pohl, C., and J. L. Van Genderen. "Review Article Multisensor Image Fusion in Remote Sensing: Concepts, Methods and Applications," International Journal of Remote Sensing 19 (5), 823–54 (2008).
[18] Reigber, A., M. Jager, W. He, L. Ferro-Famil, and O. Hellwich. "Detection and Classification of Urban Structures Based on High-Resolution SAR Imagery," In Urban Remote Sensing Joint Event, 2007, 1–6 (2007).
[19] Soergel, U., U. Thoennessen, A. Brenner, and U. Stilla. "High-Resolution SAR Data: New Opportunities and Challenges for the Analysis of Urban Areas," IEE Proceedings - Radar, Sonar and Navigation 153 (3), 294 (2006).
[20] Sonobe, Rei, Hiroshi Tani, Xiufeng Wang, Nobuyuki Kobayashi, and Hideki Shimamura. "Random Forest Classification of Crop Type Using Multi-Temporal TerraSAR-X Dual-Polarimetric Data," Remote Sensing Letters 5 (2), 157–64 (2014).
[21] Stasolla, M., and P. Gamba. "Spatial Indexes for the Extraction of Formal and Informal Human Settlements From High-Resolution SAR Images," IEEE Journal of Selected Topics in Applied Earth Observations and Remote Sensing 1 (2), 98–106 (2008).
[22] Stilla, U., U. Soergel, and U. Thoennessen. "Potential and Limits of InSAR Data for Building Reconstruction in Built-up Areas," ISPRS Journal of Photogrammetry and Remote Sensing, Algorithms and Techniques for Multi-Source Data Fusion in Urban Areas 58 (1–2), 113–23 (2003).
[23] Taubenböck, H., and N. J. Kraff. "The Physical Face of Slums: A Structural Comparison of Slums in Mumbai, India, Based on Remotely Sensed Data," Journal of Housing and the Built Environment 29 (1), 15–38 (2013).

[24] Waske, Björn, Sebastian van der Linden, Carsten Oldenburg, Benjamin Jakimow, Andreas Rabe, and Patrick Hostert "imageRF – A User-Oriented Implementation for Remote Sensing Image Analysis with Random Forests," Environmental Modelling & Software 35 (7), 192–93 (2013).